Journal of Environmental Science and Engineering B 12 (2023) 75-91
doi:10.17265/2162-5263/2023.02.003

Synthesis, Characterization and Phytotoxicity Assessment of Intercalated Insect Pheromone, Lignoceric Acid-Zinc Layered Hydroxide Nanohybrid

Rozita Ahmad[1], Mohd Zobir Hussein[2], Siti Halimah Sarijo[3], Wan Rasidah Wan Abdul Kadir[1] and Taufiq-Yap Yun Hin[4]

1. Forest Biotechnology Division, Forest Research Institute Malaysia, Kepong 52109, Selangor, Malaysia

2. Institute of Nanoscience and Nanotechnology, Universiti Putra Malaysia, Serdang 43400, Selangor, Malaysia

3. Faculty of Applied Science, Universiti Teknologi MARA, Shah Alam 40540, Selangor, Malaysia

4. Chemistry Department, Faculty of Science, Universiti Putra Malaysia, Serdang 43400, Selangor, Malaysia

Abstract: A long chain insect pheromone for subterranean termites, LC (Lignoceric Acid), was intercalated into the inorganic interlayer, ZLH (Zinc Layered Hydroxide), resulting in the formation of a new nanohybrid, labelled as LCN (Lignocerate Nanohybrid). The formation of this inorganic-organic structure nanohybrid was synthesized by the co-precipitation method using ZnO (Zinc Oxide) as the starting material. The PXRD (Powder X-Ray Diffraction) results confirmed the intercalation process although the diffraction patterns of the resultant nanohybrid and the unbound pheromone were fairly similar but both have different basal spacings values. The FTIR (Fourier Transform Infrared) profiles and the chemical composition test supported the intercalation process with the percentage loading of LC into ZLH calculated to be 85%. The thermal stability of the free anion, LC was enhanced when it was transformed into LCN, increasing from 257 ℃ to 352 ℃. The release of LC from the nanohybrid behaved in a sustained manner, governed by the pseudo-second order kinetic model with higher release of LC in sodium carbonate solution than the pH aqueous media. The synthesized nanohybrid was found to be safe for plant germination when the two seed types were successfully germinated in all the tested nanohybrid concentrations. However, the percentage seed germination and the radical seed length from the nanohybrid showed lower values compared to its counterpart anion, LC.

Key words: Insect pheromone, ZLH, ZnO, controlled release, termite.

1. Introduction

Termites have been reported worldwide as pest in wood structures and plantation of forest trees. The removal of chlorodane and other pesticide for pest control has led to search for effective, environmentally friendly compound with antitermite activity [1]. Insect pheromone is chemical substances used as attractant for insect. They are applied in fields for pest control by manipulating the insect mating activity, keeping the male species away from female and luring them to a trap. The disadvantage of chemical pesticide, is that insect can create resistance over time and this leads to producing chemicals with stronger resistance. Furthermore, the increasing use of chemical pesticide in agricultural activities will pose negative effect on environment pollution and human health. Due to this reason, insect pheromone has been of interest to be employed as one of the alternatives to chemical pesticide in agriculture application.

However, insect pheromone has some drawbacks; some easily degrade and decompose by environment such as heat and sunlight [1]. For this purpose, various controlled release material has been developed to protect the compound from degradation and at the same

Corresponding author: Rozita Ahmad, research fields: industrial chemistry, ChM, soil chemistry.

time prolong the delivery period. The controlled release formulation would not only minimise the environment related problem such as leaching and contamination but would also reduce the frequency of application as the compound is released in smaller amount over duration of time. A great interest has been focused on clay minerals and LMHs (Layered Metal Hydroxides) as controlled release formulation. LMH derived from a brucite-like structure of $Mg(OH)_2$, a hydrotalcite-like compound, is an interesting host material for delivery system of many beneficial agents such as drugs [2], herbicides [3], catalyst [4], UV-absorber [5], corrosion inhibitor [6], DNA (Deoxyribonucleic Acid) [7], flame retardant [8] and sensors [9]. This is due to their unique structure which comprised of positively charged inorganic layers allowing the anionic functional compounds to be stored between the interlayer region to form inorganic-organic composite material. Intercalation of active agent in the inorganic layer protects them from degradation and further extends the duration action of the functional agents through controlled release mechanism thus minimizing the chemical levels in the environment. These interesting properties give ZLH (Zinc Layered Hydroxide) a huge opportunity as host carrier of many beneficial agents towards developing nanostructure material with improved properties and safer environment. There are various routes for the intercalation of anion into LMH such as ion-exchange [10], structural memory effect [11, 12], hydrothermal [13] and urea hydrolysis method [14]. The co-precipitation method is one of the common methods used in the synthesis of LMH nanohybrid due to ease of preparation, fewer chemicals and having normal laboratory apparatus [15, 16]. In this study we employ the co-precipitation method to insert insect pheromone into ZLH interlayers to form ZLH intercalation compound.

This study will be carried out to encapsulate LC (Lignoceric Acid), an insect pheromone for subterranean termites into the matrix of inorganic ZLH. LC is found in wood tar, various cerebrosides and small amount in most natural fat. The formation of semiochemical nanohybrid using ZLH as the host in controlled release formulations, will result in the chemical to be used more effectively as well as safer for direct user and environmentally friendly. To date, work on ZLH as host inorganic layer for insect pheromone is still new. Previous studies on ZLH were more focused on aromatic type of beneficial agents as the intercalation anion inside ZLH nanocomposite. In this present study we report on the intercalation of long chain aliphatic insect pheromone, namely LC with ZLH for the formation of a new inorganic-organic nanocomposite, ZLH-LCN (Zinc Layered Hydroxide-Lignocerate Nanohybrid). The nanohybrid is prepared through co-precipation method using ZnO (Zinc Oxide) as source of ZLH and this paper further evaluates its physico-chemical properties, phytotoxicity and controlled release behavior.

2. Materials and Method

2.1 Synthesis of Nanohybrid

A known weight of LC was heated to melt on a hotplate at 85 ℃. Ethanol of 50 mL was added and heated to dissolve the chemical. ZnO of 0.1 g was dispersed in 50 mL deionized water for 15 min on a magnetic stirrer. The lignoceric solution of 0.025, 0.05, 0.08, 0.1 and 0.12 M was individually added slowly into ZnO water suspension with constant stirring, producing a clear solution. The pH of the solution was adjusted to 7.9 with 0.5 M NaOH aqueous solution to obtain white precipitate. The slurry solution was vigorously stirred on a magnetic stirrer for 3 h and the aging process was further continued at 70 ℃ for 18 h. The obtained material was centrifuged, thoroughly washed with deionized water and dried in an oven at 70 ℃. The obtained material was then powdered for further use and characterization. Different amount of 0.05, 0.1 and 0.25 g ZnO was used in the nanohybrid synthesis.

2.2 Characterization

Powder X-ray diffraction patterns of nanohybrid was obtained at 2-60 ° on a Shimadzu diffractometer XRD-6000 using CuK_α radiation (λ = 1.5418 Å) and dwell time of 4 °/min. FTIR (Fourier Transform Infrared) spectra were recorded over the range, 400-4,000 cm^{-1} on a Perkin Elmer, 1725X Spectrophotometer using the KBr disc method. The carbon and hydrogen composition were analysed by a carbon, hydrogen, nitrogen and sulphur (CHNS) analyzer, model Thermofinnigan Flash 2000 series. The amount of Zn in the sample was extracted with mineral acids and its concentration was determined by a Varian 725-OES inductively coupled plasma-optical emission spectrometer. Thermogravimetry and differential thermogravimetry (TGA-DTG) measurements were recorded using a Mettler Toledo instrument at a heating rate of 10 °/min in the range of 28-1,000 ℃. The surface morphology of the synthesized nanohybrid was captured on a Field emission scanning electron microscope, model JEOL JSM-7600. Surface characterization of the synthesized product was carried out using the nitrogen gas adsorption method at 77 K on a Micromeritries ASAP 2000. The sample was degassed in an evacuated heated chamber at 100 ℃, overnight.

2.3 Controlled Release Study

The controlled release study of LC from the nanohybrid into the media solution was determined using aqueous solution of sodium carbonate 0.0025, 0.005 and 0.01 M. Aqueous solutions with pH of 4 and 8 were also tested for the controlled release studies. About 2 mg of the intercalated compound was contacted with 3.5 mL of aqueous solution and the accumulated amount of LC released into the solution was recorded at 205 nm using a Perkin Elmer UV-Visible spectrophotometer, Lamda 35. The LC release kinetics was fitted to the first, pseudo-second order kinetics and parabolic diffusion models to evaluate its release mechanism.

2.4 Phytotoxicity Study

The phytotoxicity study was carried out on two types of seeds using method adopted by Keeling et al. [17]. Different amount of nanohybrid, 0.01 g, 0.1 g and 1 g and 100 mL distilled water were respectively mixed and shaked on an orbital shaker for 1 h. The solution was filtered through a Whatman filter paper no. 1. The filtered solution of 3 mL was pipetted on a filter paper Whatman no. 1 containing 15 seeds of green beans and wheat in a petri dish, respectively. The petri dish was covered to avoid loss through evaporation and placed in an incubator at 28 ℃ for 48 h. This study was also carried out using distilled water, ZnO and LC as control. As a comparison to LCN, a series concentration of 0.01 g/100 mL, 0.1 g/100 mL and 1 g/100 mL containing the unbound anion (LC) and ZnO, respectively, were conducted and then tested on the two seeds.

3. Results and Discussion

3.1 Powder X-Ray Diffraction Analysis

Fig. 1 illustrates the powder X-ray diffraction patterns of pure LC, ZnO and LCN nanohybrid synthesized at various concentrations (0.025-0.12 M). Two different diffraction patterns were observed for the unbound anion, LC (Fig. 1a). The first series of peaks at 19.6, 11.8 and 8.3 Å corresponds to 3 harmonics at 2θ = 4.5 °, 7.5 °, 10.6 °, respectively. The second peak series with sharp diffraction in contrast were detected at 18.8, 11.4, 8.2 and 6.4 Å giving up to 4 harmonics at 2θ = 4.7 °, 7.8 °, 10.8 ° and 13.9 °, respectively. These two reflection peaks are due to the existence of the interlayer domains containing anion LC species with slightly different arrangement [18]. The starting material ZnO, known to be high crystalline, portrays five sharp peaks of 100, 002, 101,102 and 110 reflections in the 2θ, between 30 ° and 40 ° as shown in Fig. 2a.

The PXRD (Powder X-Ray Diffraction) profiles of the intercalated material, LCN synthesized at 0.025 to 0.12 M of LC (Fig. 2a) show two series of diffraction

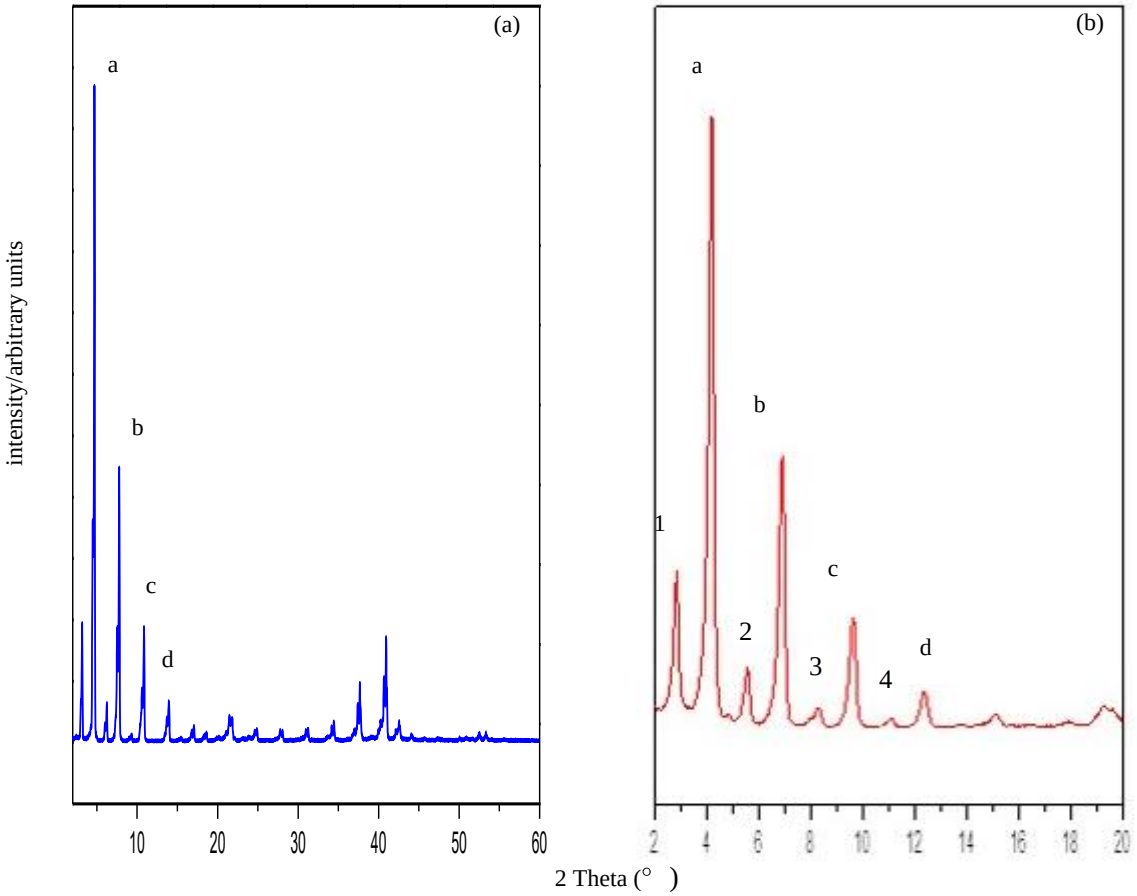

Fig. 1 PXRD profiles of (a) raw LC, d-basal spacings: 1 = 19.6 Å, 2 = 11.8 Å, 3 = 8.3 Å, a = 18.8 Å, b = 11.4 Å, c = 8.2 Å, d = 6.4 Å and (b) LCN prepared at 0.10 M LC (slow scan), d-basal spacings: 1 = 31.5 Å; 2 = 16.0 Å, 3 = 10.7 Å, 4 = 7.2 Å, a = 21.3 Å, b = 12.9 Å, c = 9.2 Å, d = 4.6 Å.

peak arrangements similar to its counterpart anion, LC, but reduce in peak intensities and have different d-basal spacing with shifted 2θ. Nanohybrid synthesized at lower concentrations, 0.025 to 0.08 M of LC shows the presence of ZnO peaks, which indicate the incomplete transformation of ZnO into layered metal hydroxide. The ZnO phase was progressively reduced as the concentration increases. At 0.10 M concentration of LC, the ZnO phase subsided indicating the pure phase of the nanohybrid. The nanohybrid synthesized at this concentration showed a well ordered nanohybrid structure. The first peak series were observed at 31.5, 16.1 and 10.7 Å reflecting up to 3 harmonics at 2θ = 2.8 °, 5.5 °and 8.2 °, respectively. This is depicted in Fig. 1b for PXRD slow scan as well as in Fig. 2a. The second peak arrangement showed 4 harmonics contributed from basal spacings of 21.3, 12.9, 9.2 and 7.2 Å at 2θ = 4.1 °, 6.8 °, 9.6 ° and 12.3 °, respectively. Further increase in the concentration to 0.12 M showed a broader peak with weak ZnO reflections. Different amount of ZnO (0.05, 0.10 and 0.15 g) was used for the synthesis of nanohybrid at 0.1 M LC. PXRD patterns in Fig. 2b show that when 0.05 and 0.15 g ZnO were applied in the preparation of nanohybrid, the presence of ZnO phase can be seen. However, when 0.1 g ZnO was used in the synthesis, the obtained material showed symmetric peaks with the highest d-basal spacing of 31.5 Å and absence of ZnO reflection. This suggests that successful intercalation of LC into the ZLH has occurred. FTIR, elemental and thermogravimetric and differential thermogravimetry analyses were carried out to verify the intercalation process of LC and will be

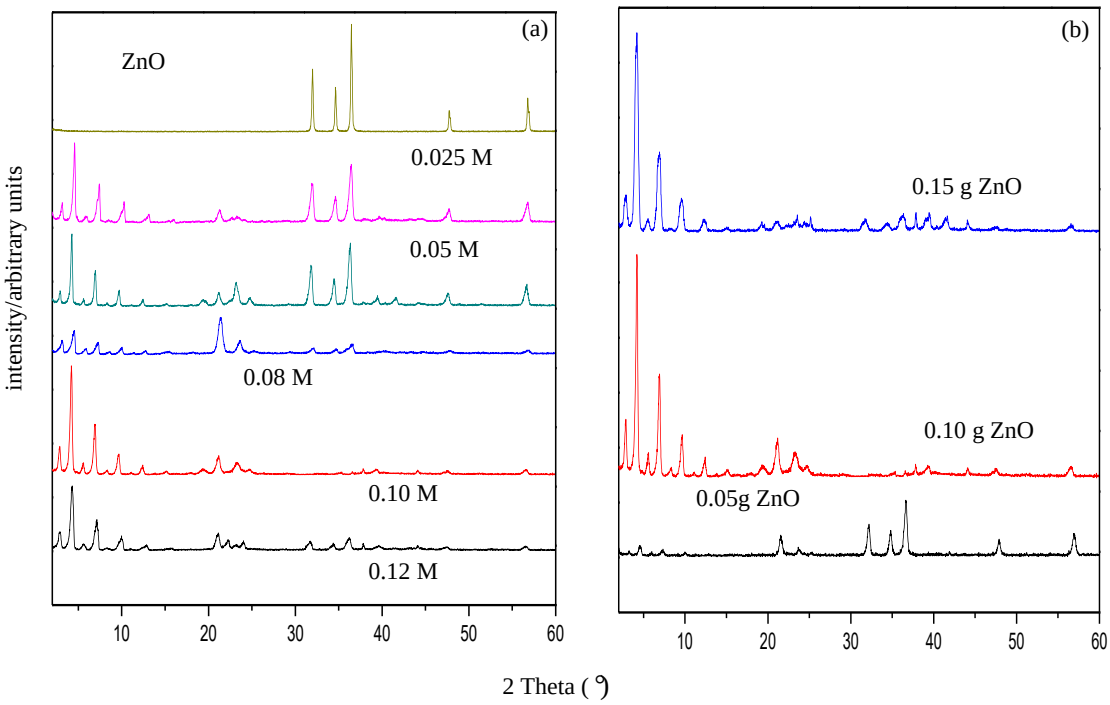

Fig. 2 PXRD patterns of ZnO and LCN prepared at 0.02, 0.05, 0.08, 0.10 and 0.12 M LC with 0.1 g ZnO (a) and LCN synthesized at 0.10 M LC using 0.05, 0.10 and 0.15 g ZnO (b).

discussed later. This nanohybrid prepared using 0.1 M LC with 0.1 g ZnO was further used for controlled release and phytotoxicity studies.

3.2 FTIR Results

The FTIR spectra for pure LC and its nanohybrid, LCN are depicted in Fig. 3 and the summary of the bands is shown in Table 1. The FTIR spectrum of pure anion exhibits a sharp band at 1,713 cm^{-1} corresponding to the C=O stretching of the carboxylates [19]. The presence of a small broad band at 3,034 cm^{-1} is assigned to the OH vibration of carboxylic group and band at 1,276 cm^{-1} is related to the C-C-O stretching. It is observed that most of the typical bands of pure LC are also found in the FTIR spectrum of its nanohybrid, LCN which suggests the intercalation of LC anion into ZLH inorganic interlayer. However, some of the bands are slightly shifted from the original position in pure LC as a result of the interaction of LC anion with the host structure, ZLH. This is observed for bands from C-H stretching of methylene symmetric and asymmetric group, and CH_2 bending which are slightly shifted from 2,911, 2,846 and 719 cm^{-1} in LC to 2,917, 2,849 and 723 cm^{-1} for LCN, respectively.

Some of the bands that exist in the pure LC disappeared in the FTIR spectrum of LCN. This is observed for bands at 1,713 and 1,276 cm^{-1} which cannot be found in the synthesized nanohybrid due to the intercalation process in which the hydrogen ions in the LC molecules are removed and that LC anion was attached to the positively charged inorganic ZLH interlayers. On the other hand, three new bands are found in the produced nanohybrid. Two new peaks at wavenumber 1,596 and 1,416 cm^{-1} are attributed to the asymmetric and symmetric of COO^-, respectively [20, 21] and one small band at 520 cm^{-1} is designated to Zn-OH of ZLH band at 3,455 cm^{-1} which contributed to the OH stretching in carboxylic group. This indicates successful intercalation of the guest anion, LC and the result is further supported by the thermogravimetric and differential thermal and elemental analyses.

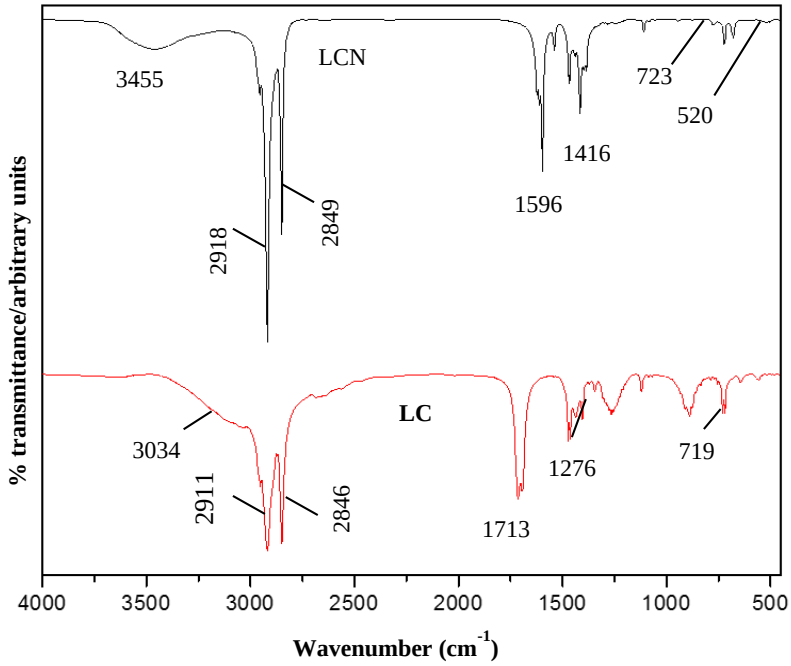

Fig. 3 FTIR spectrum of LC and LCN.

Table 1 FTIR absorption bands with functional group assignment for LC and LCN.

Assignments	LC	LCN
Vibration (O-H)	3,034	3,455
CH stretching of methyl and methylene group	2,911, 2,846	2,917, 2,849
υ (C=O) in COOH	1,713	-
Vibration (COO^-)	-	1,596 (asym), 1,416 (sym)
Zn-O, Zn-OH		520
υ (C-O) in carboxylic group	719	723
C-C-O strectching	1,276	

3.3 Thermal Analysis

The thermogravimetry and differential thermogravimetry (TGA-DTG) thermograms obtained for ZnO, free LC and its intercalated compound, LCN are shown in Fig. 4. Thermal analysis for ZnO shows small weight decomposition of 0.4% at 250 ℃, indicating high stability of the starting material. LC reported total decomposition with single weight loss of 99.8% with DTG peak at 256.8 ℃. TGA-DTG for LCN shows three major weight losses at temperature between 350 and 840 ℃. The first step of weight loss occurs at maxima temperature of 352.7 ℃, is due to the collapse of the inorganic layer, the release of water and decomposition of organic moiety LC at the interlayer domain with total loss of 42.5%. The second stage of weight loss amounted up to 41.9% is observed at maximum temperature of 451.4 ℃ due to the decomposition of the released anions. The last weight loss of about 9.4% at maximum temperature of 837.6 ℃ is related to the decomposition of carbonaceous residues provided by the intercalated species [13]. High temperatures of the dehydroxylation of the ZLH layer and decomposition of lignocerate anions in the intercalated compound, LCN are related to the strong interactions between the host layers and guest, LC [22]. This reveals that the thermal stability of LC is enhanced when it is transformed into intercalated compound, LCN.

The elemental analysis by CHNS and ICP of the nanohybrid is one of the methods applied to confirm the

intercalation of anion into ZLH interspacings. Table 2 shows the results of the elemental analysis of LCN, indicating that the nanohybrid contains 66.2% carbon and 5.8% Zn. Using the percentage carbon, the percentage anion loading is calculated to be 84.7%. The percentage anion loading of LCN gave an indication of the degree of intercalation of LC anion in the ZLH interlayer spacing [23]. This corresponds to the results obtained from the TGA/DTG analysis with the first and second weight losses amounted to 84.3%. High percentage of LC in the nanohybrid of more than 80%, could be related to the existence of anion in the outerlayer as well in the interlayer region of the host layer, ZLH.

Table 2 Physico-chemical properties of ZnO and LCN.

Sample	C (%)	Zn (%)	Anion loading (%)	BET (Brunauer-Emmett-Teller) surface area (m^2/g)	BJH (Barret-Joyner Halenda) pore diameter (Å)	Total pore volume (cm^2/g)
LCN	66.2	5.8	84.7* (84.3)**	6.9	241	0.060
ZnO	-	80.3	-	5.9	111	0.049

Estimated from CHNS *; obtained from TGA/DTG analysis **.

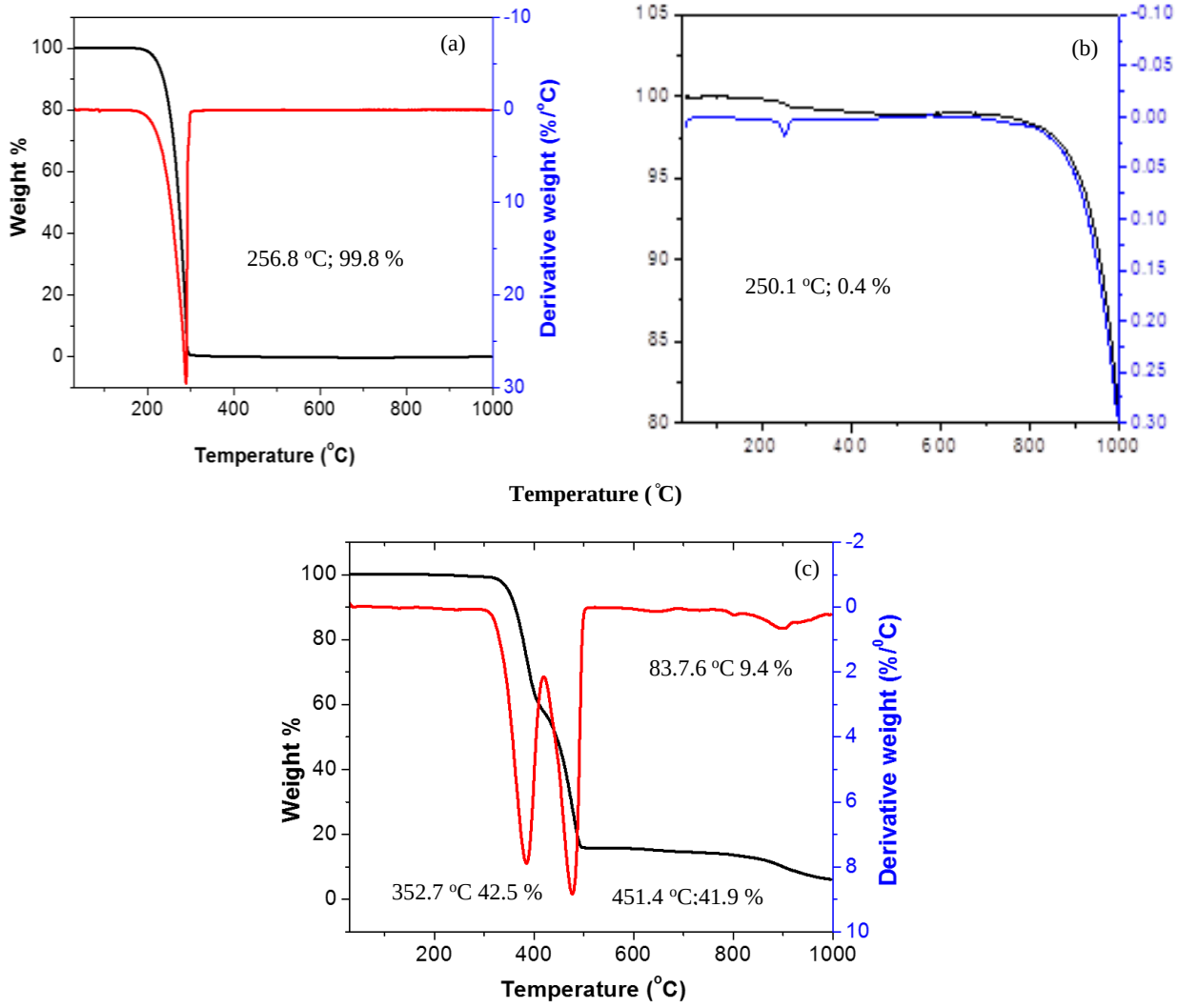

Fig. 4 TGA-DTG thermograms of the guest anion LC (a), ZnO (b) and lignocerate-ZLH nanohybrid (c).

3.4 Structural Orientation of the Guest Anion in the ZLH

Fig. 5 shows the proposed spatial arrangement of lignocerate within the ZLH interlayer region. The molecular size of LC was calculated using Chemoffice software Ultra, 2008 with the *x*, *y* and *z* axes obtained as 3.0, 22.5 and 3.4 Å, respectively The d-spacing of intercalated compound LCN from PXRD spectrum is 31.5 Å. Considering the thickness of ZLH and water molecule 4.8 and 2.6 Å, respectively, the gallery height to be occupied is 23.7 Å which is larger than 22.5 Å dimension of LC. Therefore, it is proposed that the LC anion to be positioned between the interlayers as monolayer arrangement oriented from *z*-axis as depicted in Fig. 5b. The carboxylate groups of LC were bonded through an oxygen atom to Zn^{2+} units of the lattice [24].

3.5 Surface Properties

The morphologies of ZnO, pure LC and the synthesized nanohybrid, LCN were determined using a field emission scanning electron microscope and the images are shown in Fig. 6. The micrograph of ZnO shows hexagonal and square-like structure with various shapes and sizes. Pure LC shows a plate-like morphology with various sizes and is transformed into non-uniform shape without specific structure when the nanohybrid, LCN is produced. The change of the morphology is due to the transformation of ZnO into lamellar structure and intercalated with the LC anion.

Fig. 7 shows the nitrogen adsorption-desorption isotherms of ZnO and the nanohybrid, LCN while their surface properties are listed in Table 3. The inset in Fig. 6 represents each of the pore size distribution patterns of ZnO and LCN. All the isotherms featured the Type IV isotherm with H3-type hysteresis loop according to the IUPAC (International Union of Pure and Applied Chemistry) classification. This type of isotherm profile shows rapid absorption increase at low relative pressure followed by a slow uptake and a continued rapid increase near the saturated pressure > 0.8 cm^3/g. The formation of LCN has slightly increased the BET surface area from 6 m^2/g for ZnO to 7 m^2/g when LC anion was intercalated between the interlayers of ZLH.

The change in BET surface area could be related to the increase in the particle size (BJH pore diameter) and pore volume. The intercalation process has resulted an

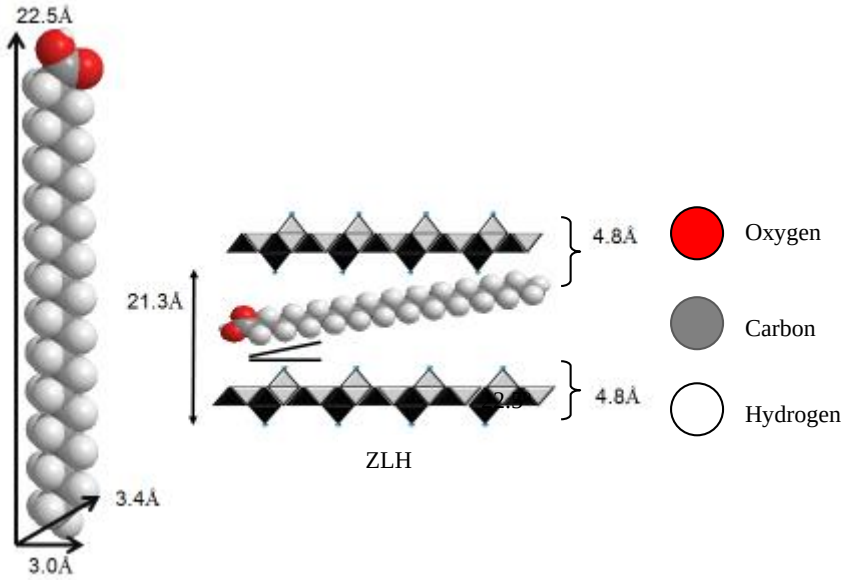

(a) (b)

Fig. 5 Three dimensional molecular structure of LC (a) and spatial orientation of LC in ZLH inorganic intergallery (b).

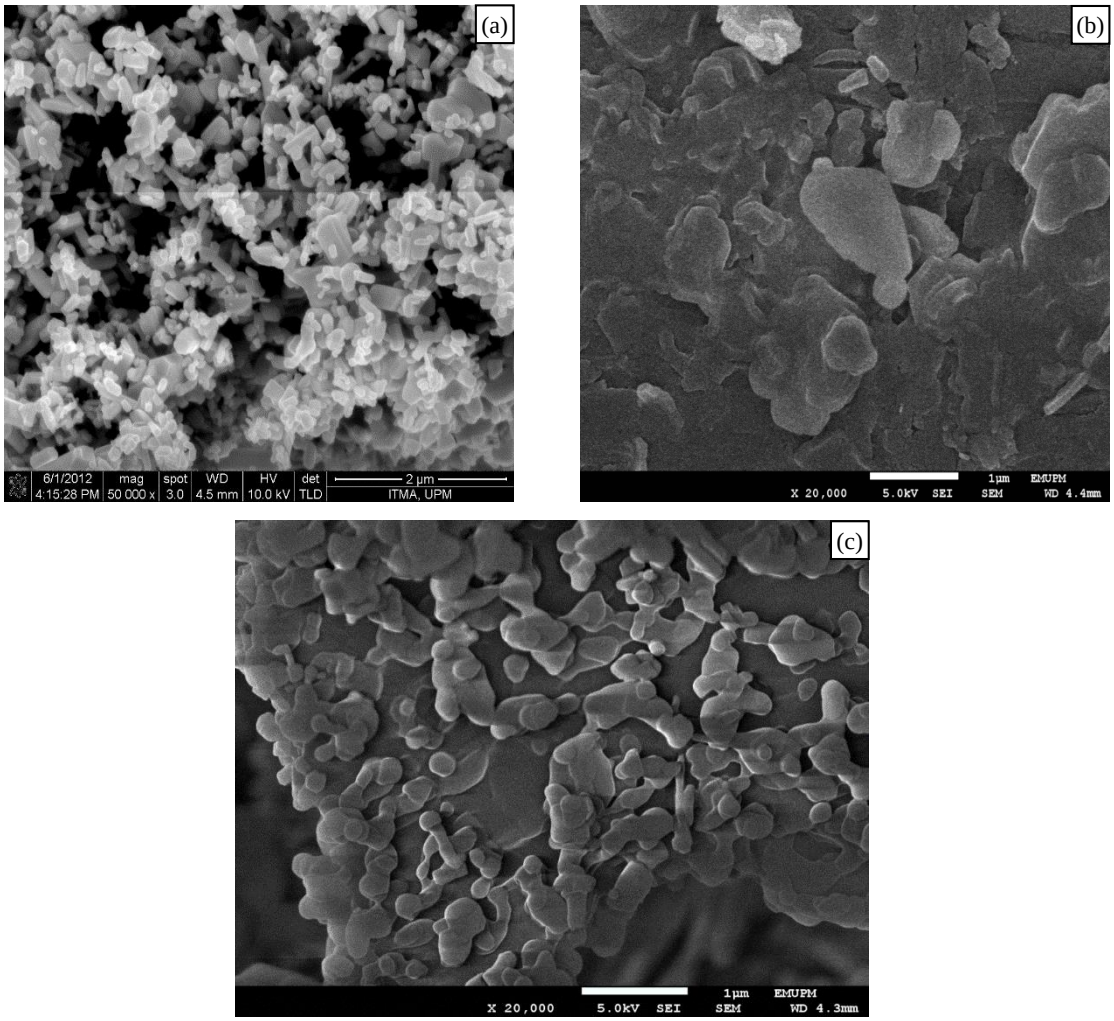

Fig. 6 Field emission scanning microscopes images of ZnO at 50,000× magnification (a), pure LC (b) and LCN (c) at 20,000× magnification.

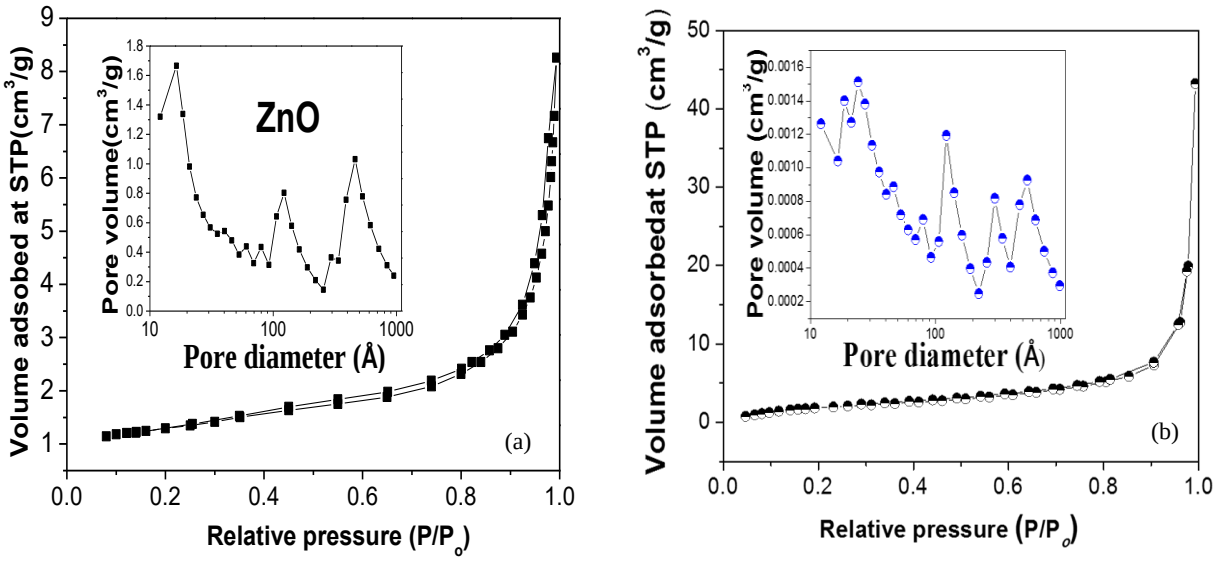

Fig. 7 Adsorption-desorption isotherms of ZnO (a) and LCN (b).
Inset shows the pore size distribution for ZnO and LCN, respectively.

increase in the BJH pore diameter from 111 for ZnO to 241 Å for LCN, and a small change in pore volume from 0.05 (ZnO) to 0.06 cm^2/g (LCN). BJH pore size distribution for ZnO and LCN shows that their pore diameter peaks are within 20-500 Å, which corresponds with the adsorption isotherm of Type IV material which represents the mesoporous and non-porous material (20-500 Å) [25].

3.6 Release Behavior of Anion from the Nanohybrid into the Release Media

3.6.1 Sodium Carbonate Solution

The release profiles of lignocerate from its nanohybrid, LCN, were obtained in sodium carbonate aqueous solution at 0.0025, 0.005 and 0.01 M concentrations as shown in Fig. 8. The release of the guest anion was found to be rapid in the beginning of the process in the first 100 min followed by a sustained release in all the sodium carbonate solutions. The release behavior of LC is due to the anion-exchange process, in which the LC anions in the interlayer of ZLH are exchanged with the carbonate anions in the release media. The ion exchange process that was faster at the early stage is due to the higher amount of carbonate in the solution which has led to higher release of the guest anion [26].

It was observed that the nanohybrid contacted in 0.01 M concentration gave higher percentage release up to 64% compared to 0.0025 and 0.005 M media with percentage release recorded to be 16% and 34%, respectively. The higher is the concentration of CO_3^{2-} in the release media, increases the ion exchange process and has resulted more LC anions to be released. The exchange process slowed down until the equilibrium stage was achieved around 700 min in 0.01 M concentration. However, in both 0.0025 and 0.005 M aqueous media, the anion release shows slow decline after 200 min. This could be due to the fact that high concentration in 0.01 M media provides ample supply of CO_3^{2-} for continuous ion exchange to take place. While in the other two aqueous solutions, the decline in anion percentage release is due to the reduced amount of CO_3^{2-} in the solution which led to small amount of LC anion to be released.

3.6.2 pH Aqueous Solution

Fig. 9 reported the release patterns of LC anion from the ZLH inorganic layer nanocomposite into the aqueous media at pH 4 and 8. The release of LC is dependent on pH in which the percentage amount of guest anion release is higher at pH 4 than pH 8 aqueous solutions. This shows that under acidic media, ZLH is easily dissolved and releasing LC anion through dissolution of the inorganic layer. At the starting process, the release of LC anion was quick in the first 100 min followed by a slower sustained step and finally reaching to equilibrium stage around 500 min. The saturated release of LC was recorded around 2% and 4% in pH 4 and 8, respectively. The small release of LC could be attributed to the long chain structure of the anion which hindered this to happen. However, the release continues to occur in a slow manner with no indication of reduction in percentage release.

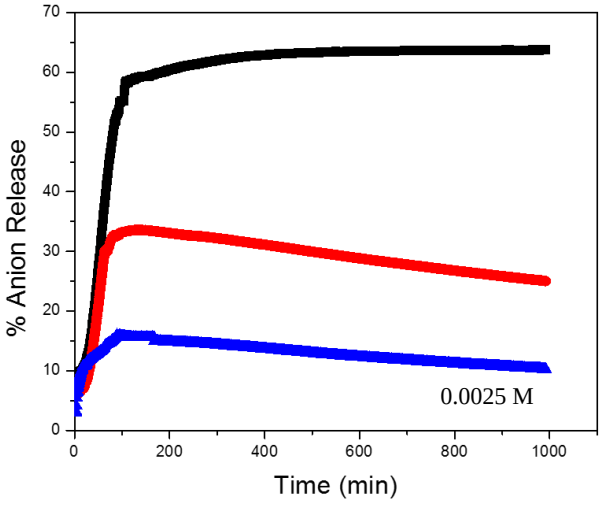

Fig. 8 Release profiles of LC from LCN interlayer into the aqueous solutions of sodium carbonate 0.0025, 0.005 and 0.01 M concentrations.

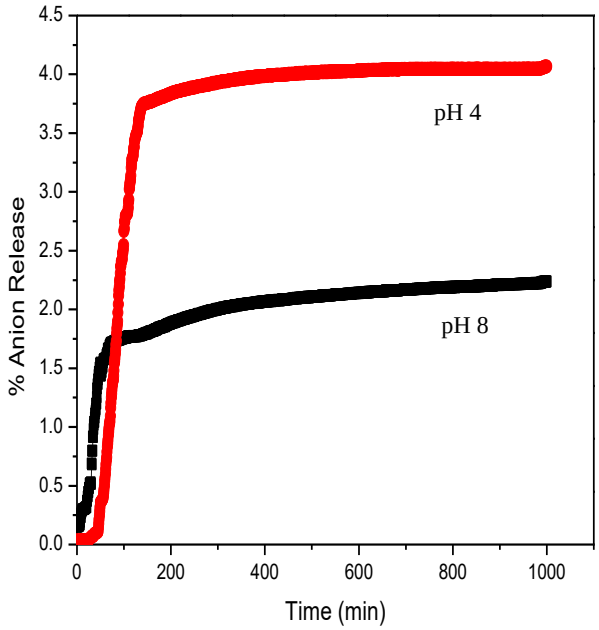

Fig. 9 Release profiles of LC from the LCN interlayer into the pH 4 and 8 aqueous solutions.

3.7 Release Kinetics of Lignocerate Anions from the Nanohybrid

The release mechanism of guest anion from the intercalated material can be described using various kinetic models. The data obtained from the controlled release study were analysed and fitted to the pseudo-first order (1), pseudo-second order (2) and parabolic diffusion (3) kinetic equations as given below:

$$\ln (q_e - q_t) = \ln q_e - k_1 t \quad (1)$$

$$t/q_t = 1/k_2 q_e^2 + t/q_e \quad (2)$$

$$(1 - M_t/M_0)/t = k\, t^{-0.5} + b \quad (3)$$

where q_e, q_t are the amount of anions released at equilibrium and at any time t, respectively and k is the release-rate constant. M_0 and M_t represent the anion remaining in the ZLH at zero time and release time t, respectively. The correlation coefficient value, R^2 obtained from the kinetic analysis is used to determine the best fit kinetic model that governs the release process of anion from the nanohybrid.

3.7.1 Release Kinetic of the Nanohybrid into Sodium Carbonate Solution

Fig. 10 represents the plots of the fitting of LC released from LCN into sodium carbonate solution. The kinetic analysis result shows that the release process was best fitted to the pseudo-second order kinetic expression with the highest R^2 values that were obtained 0.9869, 0.99930 and 0.9976 in 0.0025, 0.005 and 0.01 M sodium carbonate concentrations, respectively. The guest anion release from ZLH interspacing into sodium carbonate media could be described by the pseudo-second kinetic order through ion exchange process between the intercalated LC in the ZLH interlayer with CO_3^{2-} in the release medium [22]. The release rate values, k for LC into the three sodium carbonate media were calculated and reported in Table 3. At 0.01 M concentration, release rate value was measured to be 8.23 $\times 10^{-5}$ mg/min, compared to 1.79 and 4.80 $\times 10^{-5}$ mg/min, for 0.0025 and 0.005 M, respectively. This corresponds to the saturated anion release, the higher the release rate, more amount of anion is being released from the nanohybrid due to the high exchange anion in the release media.

3.7.2 Release Kinetic of Intercalated Anion into pH Aqueous Media

Using the kinetic equations, the release data of the intercalated LC into the pH media solution were fitted to the pseudo-second order kinetic model as shown in Fig. 11. The correlation coefficient, R^2 and the k values

Table 3 Parameters derived from the fitting of the data obtained from the release of LC from LCN intercalation compound into carbonate aqueous solution using parabolic, pseudo-first and pseudo-second order kinetic expression.

Na_2CO_3	Saturated release (%)	Correlation coefficient, R^2			Pseudo-second order
		Pseudo-first order	Pseudo-second order	Parabolic diffusion	Rate constant, k (mg/min) $\times 10^{-5}$
0.0025 M	16	0.9681	0.9887	0.9374	1.79
0.005 M	34	0.9450	0.9930	0.9252	4.80
0.01 M	64	0.8266	0.9976	0.8463	8.23

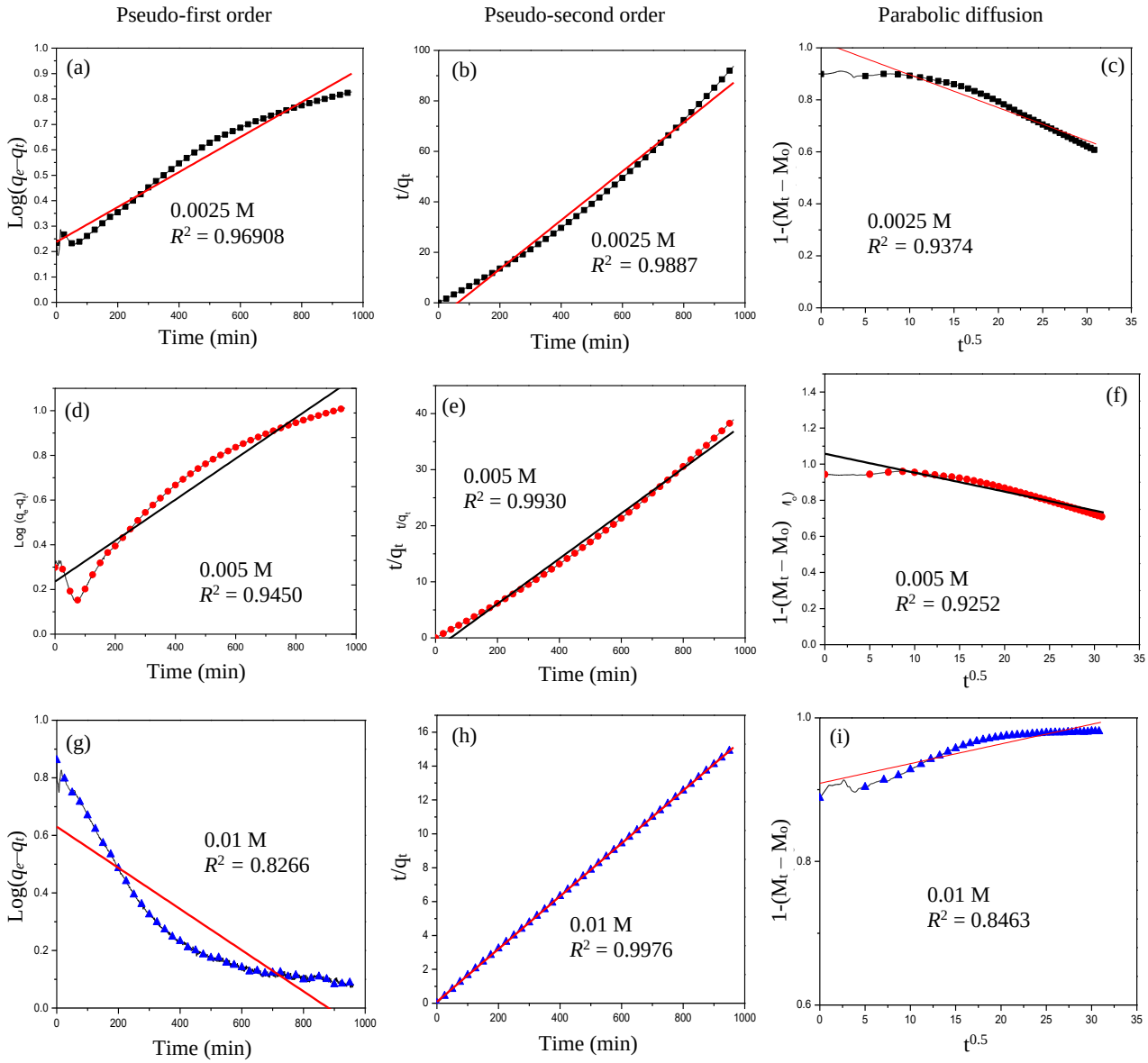

Fig. 10 Fitting the data of LC released from its nanohybrid into sodium carbonate aqueous solution using first, pseudo-second order and parabolic diffusion models at 0.0025 M (a-c), 0.005 M (d-f) and 0.0 1M (g-i) concentrations.

Table 4 Parameters derived from the fitting of the data obtained from the release of LC from LCN intercalation compound into pH 4 and pH 8 aqueous solution using parabolic, pseudo-first and pseudo-second order kinetic expression.

pH media	Saturated release (%)	Correlation coefficient, R^2			Pseudo-second order
		Pseudo-first order	Pseudo-second order	Parabolic diffusion	Rate constant, k (mg/min) $\times 10^{-5}$
4	2	0.8769	0.9938	0.9580	0.98
8	4	0.6928	0.9957	0.8315	2.32

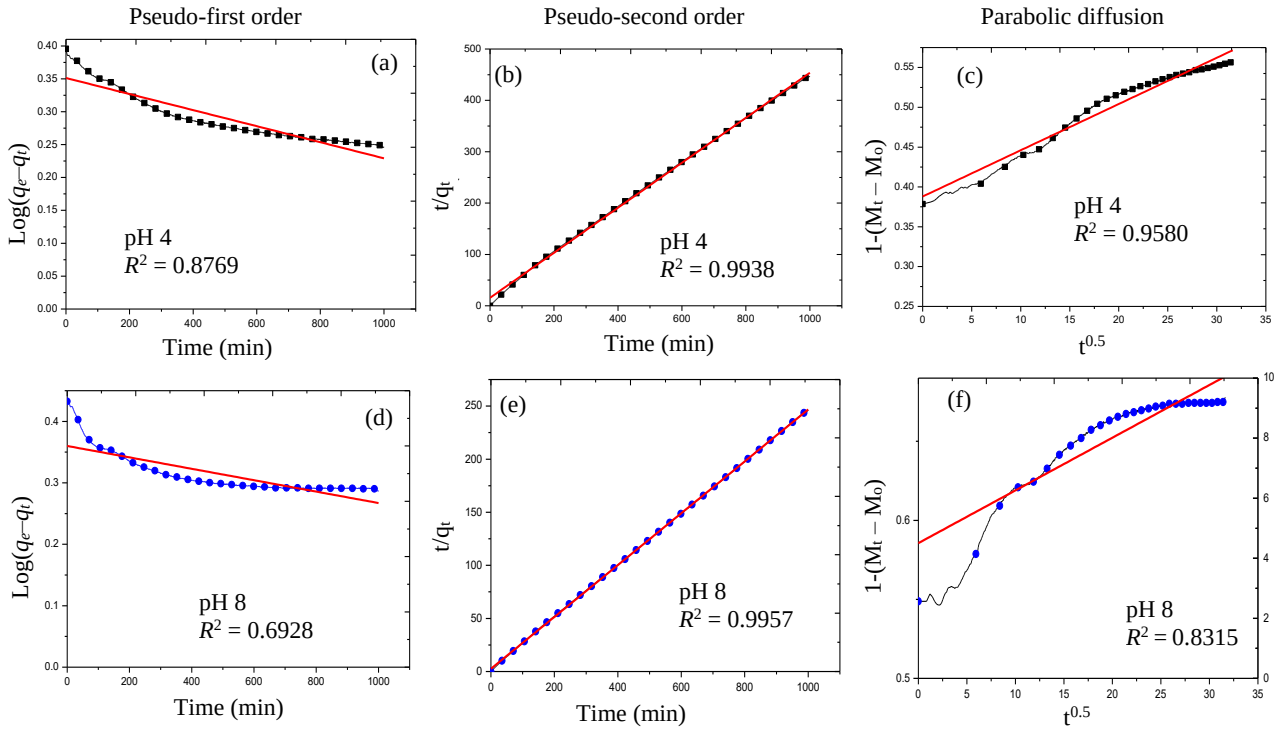

Fig. 11 Fitting the data of LC released from its nanohybrid into sodium carbonate aqueous solutions using the first-pseudo, pseudo-second order and parabolic diffusion models at pH 4 (a-c) and pH 8 (d-f).

are obtained as 0.9927 and 2.32 $\times 10^{-5}$ mg/min in pH 4 release media. At pH 8, the corresponding value is 0.9977 and 0.98 $\times 10^{-5}$ mg/min, respectively (Table 4). Most of the release process of anion such as herbicide and drug molecule intercalated into ZLH followed the similar kinetic model. The release of LC from its nanocomposite at various pH solutions was observed in a slow sustained manner governed by the pseudo-second order kinetic mechanism with the dissolution of inorganic layer. Due to the bulky structure of LC, the percentage anion release was found to be very small.

3.8 Phytotoxicity Study

3.8.1 Seed Germination Test

The phytotoxicity study of the nanohybrid was carried out through seed germination of two seed types and the results are reported in Table 5 and Fig. 12. Three controls which consisted of distilled water, ZnO and free anion, LC were tested in this experiment. The percentage germination of green beans and wheat seeds in distilled water is 91% and 82%, respectively. Treatment using ZnO increases both the germination of the two seeds with values recorded to be 93%, 96% and 98% for green beans seeds and 80%, 82% and 86% for wheat seeds at 0.01 g/100 mL, 0.1 g/100 mL and 1 g/100 mL concentration, respectively. The increase in percentage seed germination could be due to the availability of Zn from ZnO, which acts as micronutrient for plant growth.

The unbound LC shows good percentage in germination for both seed types with values of above 93%. This shows that LC can enhance seed germination and is non-toxic to plant even at higher concentration. The test using nanohybrid is found to be safe for seed germination and shows no toxic effect since all the seeds were successfully germinated. However, the intercalated LC gave lower values in percentage germination for wheat seeds with reading of 73%, 82% and 64% at 0.01 g/100 mL, 0.1 g/100 mL and 1 g/100 mL concentration, respectively and 90% in green bean seed at 1 g/100 mL concentration. This may be related to the slow release of LC from the nanohybrid material releasing the anions in a slow sustained manner as discussed in the controlled release study.

Table 5 Mean values of percentage seed germination of green beans and wheat seeds in distilled water (water), ZnO, LC and LCN at different concentrations (n = 90).

Conc. g/100 mL	Seed germination (%)							
	Green beans				Wheat seed			
	Water	ZnO	LCN	LC	Water	ZnO	LCN	LC
0	91.11 ±0.47	-	-	-	82.22 ±0.55	-	-	-
0.01	-	93.33 ±0.82	93.33 ±0.51	93.33 ±0.67	-	80.00 ±0.82	73.33 ±0.94	93.33 ±0.82
0.10	-	95.56 ±0.47	93.33 ±0.75	97.78 ±0.72	-	84.44 ±0.65	82.25 ±0.55	97.83 ±0.67
1.00	-	97.78 ±0.55	90.13 ±0.73	97.78 ±0.81	-	86.67 ±0.75	64.44 ±0.72	97.82 ±0.66

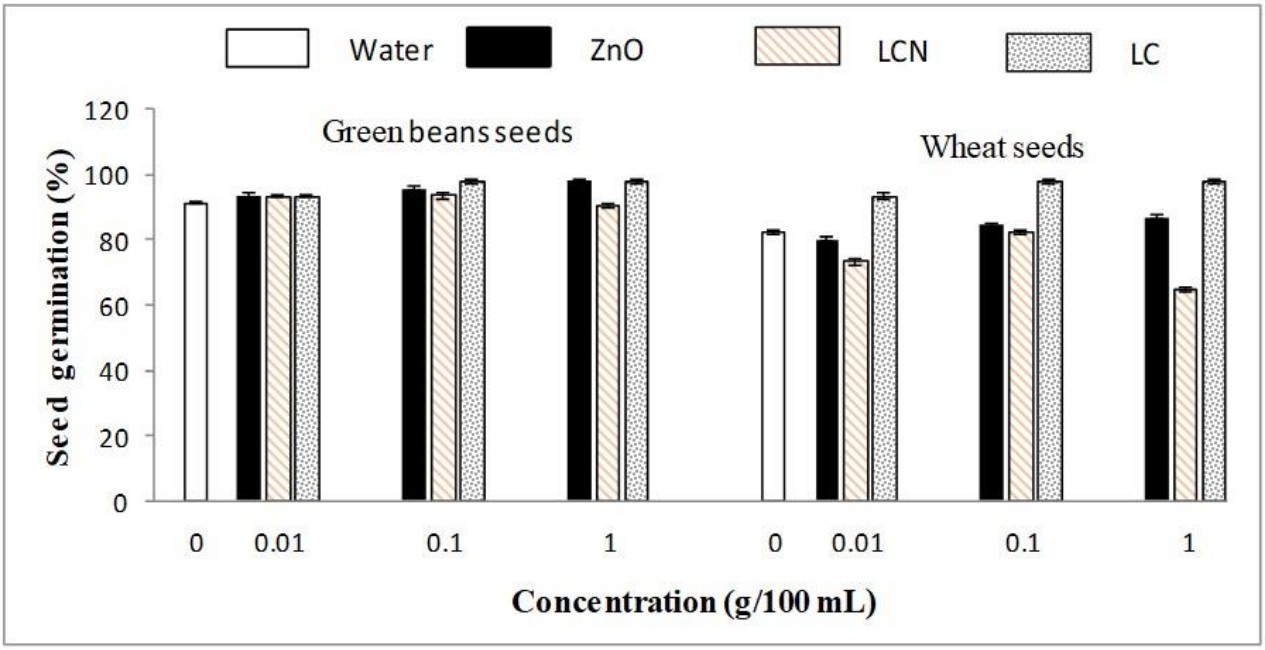

Fig. 12 Phytotoxicity of green beans and wheat seeds in distilled water (water), ZnO, lignoceric acid nanohybrid (LCN) and LC at 0.01, 0.1 and 1.0 g/100 mL concentration. The data were presented as mean ± S.D. (n = 90).

3.8.2 Evaluation on Radical Seed Length

Both seed types treated with ZnO, LCN and LC gave higher radical values compared to distilled water alone as depicted in Fig. 13. The measured length reported for distilled water is 13.26 and 9.3 mm for green beans and wheat seeds, respectively (Table 6). The radical seed length for green beans and wheat seeds increases with the increased amount of ZnO extract due to the presence of Zn which induces the radical growth. The free anion, LC was found to have good response to the radical growth on green beans which recorded the highest reading ranging from 33 to 36 mm. However, the intercalated LC shows lower radical seed length for green beans measuring 26 mm (0.01 g/mL), 23 mm (0.1 g/mL) and 31 mm (1 g/mL). This corresponds to the controlled release behavior of LCN releasing LC in small amount. Meanwhile wheat seed shows different responses in radical seed length in which both LCN and LC treatment gave similar values.

Table 6 Mean value of radical seed length of green beans and wheat seeds in distilled water (water), ZnO, LCN and LC at different levels of concentration solution (n = 90).

Conc. g/100 mL	Radical seed length (mm)							
	Green beans				Wheat seed			
	Water	ZnO	LCN	LC	Water	ZnO	LCN	LC
0	13.33 ±0.47	-	-	-	6.63 ±0.87	-	-	-
0.01	-	28.65 ±0.88	25.62 ±0.76	35.91 ±0.53	-	9.34 ±0.69	11.21 ±0.54	11.17 ±0.72
0.10	-	33.55 ±0.54	23.24 ±0.71	35.62 ±0.87	-	10.22 ±0.78	10.33 ±0.83	10.37 ±0.77
1.00	-	35.25 ±0.79	30.82 ±0.89	33.44 ±0.92	-	13.15 ±0.94	11.41 ±0.81	11.52 ±0.68

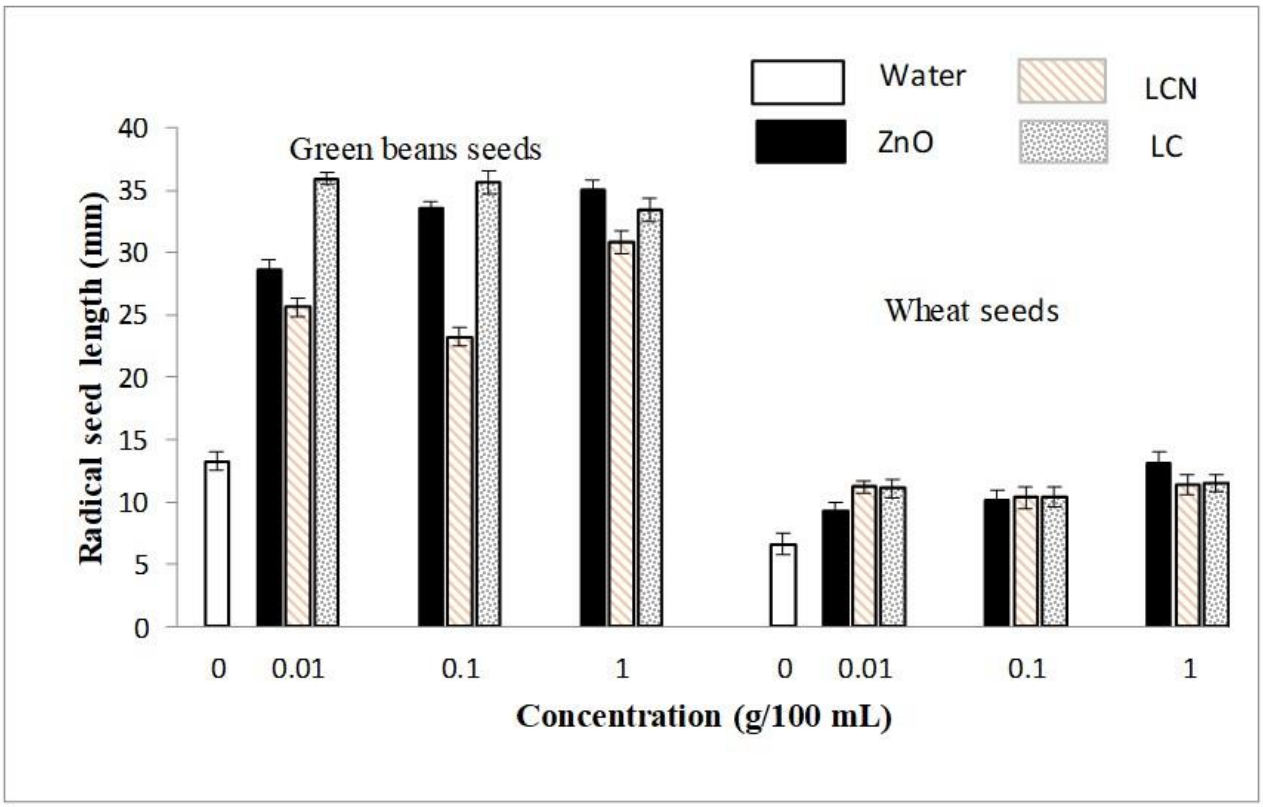

Fig. 13 Radical seed growth of green beans and wheat seeds in distilled water (water), ZnO, VAN (valeric acid nanohybrid) and VA (Valeric Acid) at 0.01, 0.1 and 1.0 g/100 mL extract solution. The results are given as mean ± S.D. (n = 90).

4. Conclusion

Intercalation of LC, a long chain aliphatic carboxylic acid into inorganic layer was obtained by a simple preparation method using ZnO as source for ZLH. The produced nanohybrid shows peak at shifted 2θ with expansion in basal spacing, confirming the intercalation process has occurred. The formation of the nanohybrid and intercalation was supported by FTIR with the presence of functional groups of LC and inorganic host. The intercalation of LC has resulted in the formation of nanohybrid with the increase in thermal stability compared to its free counterpart anion, LC. The decomposition of intercalated LC was enhanced from 257 to 353 ℃. The release behaviour of LC from its intercalated material followed the pseudo-second order model. The release of LC from the interlayer ZLH into sodium carbonate solution was found to be higher than in the pH aqueous solution. The high release of LC into sodium carbonate solution is due to the presence of CO_3^{2-} for the ion exchange to happen.

References

[1] Petroski, R. J., Tellez, M. R., and Behle, R. W. 2005. *Semiochemicals in Pest and Weed Control: An Introduction.* Washington D.C.: American Chemical Society.

[2] Gou, G. J., Liu, Y. H., Sun, Y., Huang, J., Xue, B., and Dong, L. E. 2011. "The Supramolecular Assembly and Magnetic Targeted Slow-Release Effect of 'Dextran-Magnetic Layered Double Hydroxide-Fluorouracil' Drug Delivery System." *Acta Pharmaceutica Sinica* 46: 1390-8.

[3] Ragavan, A., Khan, A., and O'Hare, D. 2006. "Selective Intercalation of Chlorophenoxyacetates into the Layered Double Hydroxides $[LiAl_2(OH)_6]Cl \cdot xH_2O$." *Journal of Material Chemistry* 16 (16): 4155-9.

[4] Nakagaki, S., Castro, K. A. D. F., Ucoski, G. M., Halma, M., Prévot, V., Forano V., and Wypych, F. 2014. "Anionic iron (III) Porphyrin Immobilized on/into Exfoliated Macroporous Layered Double Hydroxides as Calatyst for Oxidation Reactions." *Journal of Brazilian Chemistry Society* 25 (12): 2329-38.

[5] Sun, W., He, Q., and Luo, Y. 2007. "Synthesis and Properties of Cinnamic Acid Series Organic UV Ray Absorbents-Interleaved Layered Double Hydroxides." *Material Letter* 61: 1881-4.

[6] Mahajanam, P. V., and Buchheit, R. G. 2008. "Characterization of Inhibitor Release from Zn-Al-$[V10028]^{6-}$ Hydrotalcite Pigments and Corrosion Protection from Hydrotalcite-Pigmented Epoxy Coatings." *Corrosion* 64: 230-40.

[7] Li, B., Wu, P., Ruan, B., Liu, P., and Zhu, N. 2014. "Study on the Adsorption of DNA on the Layered Hydroxides (LDHs)." *Spectrochimia Acta Part A: Molecular and Biomoleclar Spectroscopy* 121: 387-93.

[8] Nyambo, C., Kandare, E., Wang, D. Y., and Wilkie, C. A. 2008. "Flame-Retarded Polystyrene: Investigating Chemical Interactions between Ammonium Polyphosphate and MgAl Layered Double Hydroxide." *Polymer Degradation and Stability* 93: 1656-3.

[9] Zhang, F. T., Long, X., Zhang, D. W., Sun, Y. L., Zhou, Y. L., Ma, Y. R., et al. 2014. "Layered Double Hydroxide-Hemin Nanocomposite as Mimeticperoxidase and Its Application in Sensing." *Sensor Actuators B. Chemistry* 192: 150-6.

[10] Morel-Desrosiers, N., Pisson, J., Israëli, Y., Taviot-Guého, C., Besse, J. P., and Morel, J. P. 2003. "Intercalation of Dicarboxylate Anions into a Zn-Al-Cl Layered Double Hydroxide. Microcalorimetric Determination of the Enthalpies of Anion Exchange." *Journal of Material Chemistry* 13: 2582-5.

[11] Gao, X., Lei, L., O'Hare, D., Xie, J., Gao, P., and Chang, T. 2013. "Intercalation and Controlled Release Properties of Vitamin C Intercalated Layered Double Hydroxide." *Journal of Solid State Chemistry* 203: 174-80.

[12] Hussein, M. Z., Ghotbi, M. Y., Yahya, A., and Abd. Rahman, M. Z. 2009. "Synthesis and Characterization of (Zinc-Layered-Gallate) Nanohybrid Using Structural Memory Effect." *Materials Chemistry and Physics* 113: 491-6.

[13] Dang, S., Yan, D., and Lu, J. 2012. "8-Hydroxypyrene-1,3,6-Trisulphonate and Octasulphonate Co-assembled Layered Double Hydroxide and Its Controllabesolid-State Luminescence by Hydrothermal Synthesis." *Journal of Solid State Chemistry* 185: 219-24.

[14] Hibino, T., and Ohaya, H. 2009. "Synthesis of Crystalline Layered Double Hydroxide: Precipitation by Using Urea Hydrolysis and Subsequent Hydrothermal Reactions in Aqueous Solutions." *Applied Clay Science* 45: 123-32.

[15] Crepaldi, E. L., Pavan, P. C., and Valim, J. B. 2000. "Comparative Study of the Coprecipitation Methods for the Preparation of Layered Double Hydroxides." *Journal of Brazillian Chemical Society* 11 (1): 64-70.

[16] Barahuie, F., Hussein, M. Z., Aruselvan, P., Fakurazi, S., and Zainal, Z. 2013. "Development of the Anticancer Potential of Clorogenate-Zinc Layered Hydroxide Nanohybrid with Controlled Release Property against Various Cancer Cells." *Science of Advanced Materials* 5: 1983-93.

[17] Keeling, A. A., Paton, I. K., and Mullet, J. A. J. 1994. "Germination and Growth of Plants in Media Containing Unstable Refuse-Derived Compost." *Soil Biology and Biochemistry* 26 (6): 767-72.

[18] Bashi, A. M., Hussein, M. Z., Zainal, Z., and Tichit, D. 2013. "Synthesis and Controlled Release Properties of 2,4-Dichlorophenoxy Acetate-Zinc Layered Hydroxide Nanohybrid." *Journal of Solid State Chemistry* 203: 19-24.

[19] Machado, G. S., Arizaga, G. G. C., Wypych, F., and Nakagaki, S. 2010. "Immobilization of Anionic Metalloporphyrins on Zinc Hydroxide Nitrate and Study of an Unusal Catalytic Activity." *Journal of Catalysts* 274: 130-41.

[20] Kenawi, I. M., Barsoum, B. N., and Youssef, M. A. 2005. "Drug-Drug Interaction between Diclofenac, Cetrizine and Ranitidine." *Journal of Pharmacy Biomedical Analysis* 37 (4): 655-61.

[21] Yuan, Q., Wei, M., Evans, D. G., and Duan, X. 2004. "Preparation and Investigation of Thermolysis of L-Aspartic Acid-Intercalated Layered Double Hydroxide." *Journal of Physical Chemistry B.* 108 (33): 12381-7.

[22] Ghotbi, M. Y., and Hussein, M. Z. 2010. "Gallate-Zn-Al-Layered Double Hydroxide as an Intercalated Compound with New Controlled Formulation of Anticarcinogenic Agent." *Journal of Physics and Chemistry of Solids* 71: 1565-70.

[23] Hussein, M. Z., Nazaruddin, N. F., Sarijo, S. H., and Yarmo, M. A. 2012. "Synthesis of a Layered Organic-Inorganic Nanohybrid of 4-Chlorophenoxyacetate-Zinc-Layaerd Hydroxide with Sustained Release Properties." *Journal of Nanomaterial* 12: 9.

[24] Newman, S. P., and Jones, W. 1999. "Comparative Study of Some Layered Hydroxide Salt Containing Exchangeable Interlayer Anions." *Journal of Solid State Chemistry* 148 (1): 1796-801.

[25] Sing, K. S. W., Everett, D. H., Haul, R. A. W., Moscou, L., Pierotti, R. A., Rouquerol, J., et al. 1985. "Reporting Physiosorption Data for Gas/Solid Systems with Special Reference to the Determination of Surface Area and Porosity." *Pure Applied Chemistry* 57 (4): 603-19.

[26] Hussein, M. Z., Yahaya, A., Zainal, Z., and Kian, L. H. 2005. "Nanocomposite-Based Controlled Release Formulation of an Herbicide, 2,4-Dichlorophenoxyacetate Incapsulated in Zinc-Aluminium-Layered Double Hydroxide." *Science Technology and Advanced Material* 6 (8): 956-962. doi: 10.1016/j.stam.2005.09.004.